

Hydrodechlorination of Chlorinated Ethanes by Nanoscale Pd/Fe Bimetallic Particles

Hsing-Lung Lien¹ and Wei-xian Zhang²

Abstract: Chlorinated ethanes are contaminants commonly found in soil and groundwater. The potential of nanoscale bimetallic (Fe/Pd) particles for the hydrodechlorination of seven chlorinated ethanes ($C_2H_{6-x}Cl_x$) was evaluated in batch experiments. Hexachloroethane (HCA) (C_2Cl_6), pentachloroethane (PCA) (C_2HCl_5), 1,1,2,2-tetrachloroethane (1,1,2,2-TeCA, $C_2H_2Cl_4$), and 1,1,1,2-tetrachloroethane (1,1,1,2-TeCA, $C_2H_2Cl_4$) were rapidly hydrodechlorinated (9–28 min half-lives) at a nanoparticle loading of 5 g/L. End products were ethane (61–87%) and ethylene (6–16%). Only one chlorinated intermediate, a corresponding β -elimination product, appeared temporarily during the reactions. Reductive dechlorination of 1,1,1-trichloroethane (1,1,1-TCA, $C_2H_3Cl_3$) to ethane was completed at a relatively slower rate with half-life at 44.9 min. Little reduction of dichloroethane ($C_2H_4Cl_2$) was observed within 24 h. The Pd/Fe bimetallic nanoparticles generally exhibit much higher reactivity when compared with conventional micro- and millimeter scale iron powders. The hydrodechlorination reactions are more complete, with a much higher yield of ethane and lower yield of chlorinated byproducts. A kinetic model incorporating a transition state species was proposed. Results from this work suggest that the Pd/Fe bimetallic nanoparticles may represent a treatment alternative for in situ remediation of chlorinated ethanes.

DOI: 10.1061/(ASCE)0733-9372(2005)131:1(4)

CE Database subject headings: Hydrocarbons; Ground-water pollution; Soil pollution; Iron; Kinetics; Remedial action.

Introduction

Chlorinated organic compounds are prevalent soil and groundwater contaminants. Chlorinated ethanes have commonly been used as cleaning solvents in drying cleaning, in semiconductor fabrication, and in various industrial applications such as the production of refrigerants, herbicides, and plastics. Chlorinated ethanes, like many other chlorinated organic compounds, have inevitably been discharged into the environment. Due to their slow biodegradation and strong sorption, chlorinated ethanes have caused widespread contamination of soil and groundwater. Recent investigations showed that chlorinated ethanes such as 1,1,1-trichloroethane (1,1,1-TCA) were among the most frequently detected volatile organic compounds in groundwater in both urban and rural areas (Squillace et al. 1999). Several of the chlorinated ethanes including hexachloroethane (HCA), 1,1,2,2-tetrachloroethane (1,1,2,2-TeCA), and 1,1,1-TCA have been listed as priority pollutants by the U.S. Environmental Protection Agency (USEPA 1979). Because of the potential threat to public health, the development of cost-effective treatment technologies is greatly needed.

We have reported the synthesis and applications of nanoscale bimetallic (Pd/Fe) particles as a remedial reagent for hydrodechlorination of various chlorinated hydrocarbons such as chlorinated ethenes, aromatics, and polychlorinated biphenyls (Wang and Zhang 1997; Zhang et al. 1998; Lien and Zhang 1999, 2001). The nanoscale metallic particles have typical diameters less than 100 nm and feature 0.1–1% by weight of palladium deposited on the surface of iron. The average specific surface area of the nanoparticles is about 33.5 m²/g, which is significantly greater than that of conventional microscale iron powder (typically <1 m²/g). The surface-area-normalized reactivity (k_{SA}) of the nanoscale Pd/Fe bimetallic particles is 1–3 orders of magnitude higher than that of conventional microscale iron particles. The high reactivity of nanoscale Pd/Fe bimetallic particles has been attributed to the large surface area and the presence of catalytic palladium on the iron surface.

The feasibility of injecting nanoscale bimetallic particles into a contaminated aquifer has been demonstrated (Elliott and Zhang 2001). A small quantity (1.7 kg) of nanoscale Pd/Fe bimetallic particles was gravity-fed into a testing zone where groundwater was contaminated with trichloroethylene (TCE) and other chlorinated solvents. Up to 96% of TCE was dechlorinated within the plume over a 4 week monitoring period. The total TCE removal was greater than 55% within a radius of 4.5 m after 8 weeks. Due to their high reactivity and small size, nanoscale bimetallic particles can serve as highly flexible remediation vehicles in a variety of environmental applications as demonstrated in the study. In addition to the in situ direct injection of nanoscale particles to promote in situ dechlorination, recent research suggests that nanoparticles could be fixed onto activated carbon, zeolite, or membrane for wastewater treatment (Zhang 2003).

Reaction kinetics and mechanisms for the transformation of various chlorinated solvents with zero-valent iron have been widely reported (Matheson and Tratnyek 1994; Orth and Gillham

¹Dept. of Civil and Environmental Engineering, Lehigh Univ., Bethlehem, PA 18015; presently, Dept. of Civil and Environmental Engineering, National Univ. of Kaohsiung, Kaohsiung, Taiwan, ROC.

²Professor, Dept. of Civil and Environmental Engineering, Lehigh Univ., Bethlehem, PA 18015 (corresponding author). E-mail: wez3@lehigh.edu

Note. Associate Editor: Mark J. Rood. Discussion open until June 1, 2005. Separate discussions must be submitted for individual papers. To extend the closing date by one month, a written request must be filed with the ASCE Managing Editor. The manuscript for this paper was submitted for review and possible publication on September 19, 2002; approved on March 5, 2004. This paper is part of the *Journal of Environmental Engineering*, Vol. 131, No. 1, January 1, 2005. ©ASCE, ISSN 0733-9372/2005/1-4-10/\$25.00.

1996; Roberts et al. 1996; Campbell et al. 1997; Fennelly and Roberts 1997; Arnold and Roberts 1998, 2000). Although it is generally accepted that the reductive dechlorination is a surface-mediated reaction, the known facts of the reactions occurring at the water–metal interface are rather limited (Weber 1996). The limitations are largely due to the difficulty of gaining direct evidence from the water–metal interface. Although extensive literature can be found on chlorinated ethenes ($C_2H_{4-x}Cl_x$), little information has been reported on the dechlorination of chlorinated ethanes ($C_2H_{6-x}Cl_x$) by zero-valent metals (Fennelly and Roberts 1997; Arnold et al. 1999). Reactions of chlorinated ethanes are generally slower and typically produce many chlorinated byproducts. As a part of our research on the treatment of diverse chlorinated hydrocarbons, this paper focuses on the transformation of chlorinated ethanes using nanoscale Pd/Fe bimetallic particles. Results on the rate and extent of transformation of chlorinated ethanes are presented. Reaction products were identified and quantified. Correlation analysis of reaction rates with one-electron reduction potential and bond strength were developed. A kinetic model addressing the significance of the surface reactions was also proposed. Evidence obtained from these analyses provides valuable insights into mechanisms of the surface reactions.

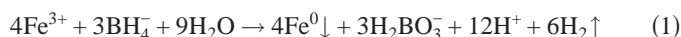
Experiment

Chemicals and Materials

HPLC grade HCA, pentachloroethane (PCA), 1,1,1,2-TeCA, 1,1,2,2-TeCA, 1,1,1-TCA, tetrachloroethylene (PCE), and trichloroethylene (TCE) were obtained from Aldrich. 1,2-Dichloroethane (1,2-DCA), 1,1-DCA, 1,1-dichloroethylene (1,1-DCE), *trans*-dichloroethylene (*trans*-DCE), *cis*-dichloroethylene (*cis*-DCE), and a standard gas mixture containing methane, ethane, ethylene, and C_3 – C_4 hydrocarbons (15 ppm each) were obtained from Supelco. Standard gases of 1.04% ethylene and 1.04% methane were acquired from Aldrich. Sodium borohydride ($NaBH_4$, 98%) and ferric chloride ($FeCl_3 \cdot 6H_2O$, 98%) were purchased from Aldrich. Palladium acetate ($[Pd(C_2H_3O_2)_2]_3$, Pd 47.4%) was from Alfa.

Preparation of Nanoscale Metal Particles

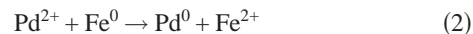
Synthesis of nanoscale iron particles was achieved by adding 1:1 volume ratio of sodium borohydride (0.25 M) into ferric chloride (0.045 M) solution. The borohydride to ferric iron ratio was 7.4 times higher than that of the stoichiometric requirement. Excessive borohydride was applied to accelerate the synthesis reaction and ensure uniform growth of iron crystals. Ferric iron was reduced by borohydride according to the following reaction (Glavee et al. 1995; Wang and Zhang 1997):



The suspension was mixed vigorously at room temperature ($22 \pm 1^\circ C$). After the $NaBH_4$ was added to the $FeCl_3$ solution, the mixture was stirred for 20 min or until visible hydrogen evolution had ceased. The metal particles formed from the above reaction have sizes generally less than 100 nm (average 66.7 nm) and an average specific surface area of $33.5 \text{ m}^2/\text{g}$ (Wang and Zhang 1997).

Nanoscale Pd/Fe bimetallic particles were prepared by soaking the freshly prepared nanoscale iron particles in an ethanol solu-

tion with 0.5% by weight of palladium acetate. This caused the reduction and subsequent deposition of Pd onto the Fe surface (Grittini et al. 1995; Wang and Zhang 1997).



Batch Experiments

Batch experiments were conducted in 150 mL serum bottles. For each serum bottle, 20 μL of chlorinated ethane stock solution prepared in methanol was spiked into a 50 mL aqueous solution containing 0.25 g of nanoscale Pd/Fe bimetallic particles (5 g Fe/L). The initial concentration of chlorinated ethanes ranged from 20 to 30 mg/L. The serum bottles were then capped with Teflon Mininert valves and mixed on a rotary shaker (30 rpm) at room temperature $22 \pm 1^\circ C$. Parallel experiments were also performed without the metal particles (control). Analyses of organic mass in the controls indicated that the total organic mass varied by less than 5% over the course of a typical experiment (< 24 h).

Analytic Methods

At selected time intervals, a 20 μL headspace gas aliquot was withdrawn using a gastight syringe for gas chromatography (GC) analysis. Concentrations of chlorinated compounds were measured by a HP5890 GC equipped with a DB-624 capillary column (J&W, $30 \text{ m} \times 0.32 \text{ mm}$) and an electron capture detector (ECD). Oven temperature was programmed as follows: hold at $50^\circ C$ for 5 min; ramp at $20^\circ C/\text{min}$ to $180^\circ C$, and hold for 5 min. Injector and detector temperatures were set at 180 and $300^\circ C$, respectively. Calibration curves for each model compound were made initially and the variability was checked before analysis ($< 15\%$). Hydrocarbon products (e.g., ethane and ethene) in the headspace were quantified with HP5890 GC equipped with a flame ionization detector and an AT-Q column (Alltech, $30 \text{ m} \times 0.32 \text{ mm}$). Constant temperatures of oven, injection, and detector were set at 30, 250, and $300^\circ C$, respectively.

Rates of Transformation

The apparent reaction rate was treated with a pseudofirst-order equation

$$\frac{dC}{dt} = -k_s C \quad (3)$$

where C = concentration of a chlorinated ethane in the aqueous phase (mg/L); k_s = observed first-order rate constant (h^{-1}); and t = time (h). Methods of standard linear regression were used to obtain the observed first-order rate constants (k_s).

Results and Discussion

Transformation of Chlorinated Ethanes

Seven chlorinated ethanes, HCA (C_2Cl_6), PCA (C_2HCl_5), 1,1,2,2-TeCA ($C_2H_2Cl_4$), 1,1,1,2-TeCA ($C_2H_3Cl_4$), 1,1,1-TCA ($C_2H_3Cl_3$), 1,2-DCA ($C_2H_4Cl_2$), and 1,1-DCA ($C_2H_4Cl_2$), were investigated for their reactions with the nanoscale Pd/Fe bimetallic particles. Rapid and complete degradation of chlorinated ethanes was achieved for HCA, PCA, TeCAs, and TCAs. However, no measurable ($< 5\%$) reduction of 1,1-DCA and 1,2-DCA was observed within 24 h. The logarithmic plots of concentration versus time

Table 1. Summary of Product Distributions, Observed Rate Constants, and Half-Lives for Transformation of Chlorinated Ethanes by Nanoscale Pd/Fe Bimetallic Particles

Chlorinated ethanes	Chlorinated intermediates	End products	k_s (h^{-1})	$t_{1/2}$ (min)
C_2Cl_6	C_2Cl_4 (7.5%), $C_2HCl_5^a$ 1,1,2,2- $C_2H_2Cl_4^a$	C_2H_6 (87%), C_2H_4 (6%)	3.43	12
C_2HCl_5	C_2HCl_3 (14%), 1,1,2,2- $C_2H_2Cl_4^a$	C_2H_6 (60%), C_2H_4 (14%)	4.46	9.3
1,1,1,2- $C_2H_2Cl_4$	1,1- $C_2H_2Cl_2$ (15%)	C_2H_6 (73%), C_2H_4 (10%)	3.60	11.6
1,1,2,2- $C_2H_2Cl_4$	<i>cis</i> - $C_2H_2Cl_2$ (10%), <i>trans</i> - $C_2H_2Cl_2$ (4.5%), 1,1,2- $C_2H_3Cl_3^a$	C_2H_6 (61%), C_2H_4 (16%)	1.51	27.5
1,1,1,- $C_2H_3Cl_3$	1,1- $C_2H_4Cl_2^a$	C_2H_6 (60%), $C_2H_4^a$	0.93	44.9

^aSuperscript *t* represents a trace amount (<1%) of the particular compound detected.

were generally linear ($r^2 > 0.97$), suggesting that the reaction can be treated as pseudofirst order. The observed rate constants and half-life are listed in Table 1. These data illustrate that the reactivity of the nanoparticles toward chlorinated ethanes is highly dependent on the degree of chlorination. Highly chlorinated ethanes (i.e., chlorine number ≥ 4) had much higher reaction rates, whereas, little reactivity was found with the lesser chlorinated ethanes (i.e., chlorine number ≤ 2).

Information on reaction intermediates and product distributions is also presented in Table 1. Comparable patterns of end product distributions were observed for the hydrodechlorination of highly chlorinated ethanes with ethane as the primary product (61–87%). Yields of ethylene were only 6–16%. For example, the disappearance of HCA corresponded with the immediate appearance of ethane and ethylene [Fig. 1(a)]. The yields of ethane and ethylene averaged 87 and 6%, respectively. Tetrachloroethylene (PCE) was the main chlorinated intermediate (7.5% at maximum) but no accumulation of PCE was found. Tetrachloroethylene is produced apparently as a result of β elimination from chlorinated ethanes to ethylene. Our previous study demonstrated that PCE can be completely dechlorinated by the nanoparticles (Lien and Zhang 2001). Trace amounts of PCA and 1,1,2,2-TeCA were detected very briefly, and were near the detection limit (<10 $\mu\text{g/L}$).

Compared with HCA, transformation of 1,1,1-TCA produced much less ethane (~60%) [Fig. 1(b)]. 1,1-DCA was the only detectable chlorinated intermediate (<1%), which was completely degraded in 2–3 h. A trace level of ethylene (<1%) appeared briefly in the headspace. It is noteworthy that reactions of chlorinated ethanes with conventional iron powders (from millimeters to micrometers) tend to produce mostly chlorinated byproducts and no ethane. Because the chlorinated intermediates are of great concern for their impact on human health and the environment, the low yield of chlorinated intermediates is a clear advantage for the use of nanoscale Pd/Fe bimetallic particles.

Correlation Analysis

Correlation analysis has been widely used to determine the relationships between molecular characteristics, thermodynamic parameters, and reaction rates (Johnson et al. 1996; Scherer et al. 1998; Burrow et al. 2000; Liu et al. 2000). It is commonly used to predict the reactivity of contaminants as well as to understand the underlying reaction mechanisms. For example, an excellent correlation has been found between the reaction rate and the one-electron reduction potential for the dechlorination of chlorinated ethylenes with zero-valent iron (Arnold et al. 1999). Other methods of correlation include linear free energy relationships and/or

quantitative structure–activity relationship based upon bond strength and lowest unoccupied molecular orbital energy.

Due to the small size and large surface area of the nanoparticles, the surface-area-normalized rate constant has been shown to be a useful tool to compare the results in the literature which has been typically generated with much larger iron particles (Johnson et al. 1996)

$$k_{SA} = \frac{k_s}{a_s \rho} \quad (4)$$

where k_{SA} = surface-area-normalized rate constant ($L/h/m^2$); a_s = specific surface area of metal (m^2/g); and ρ = mass concen-

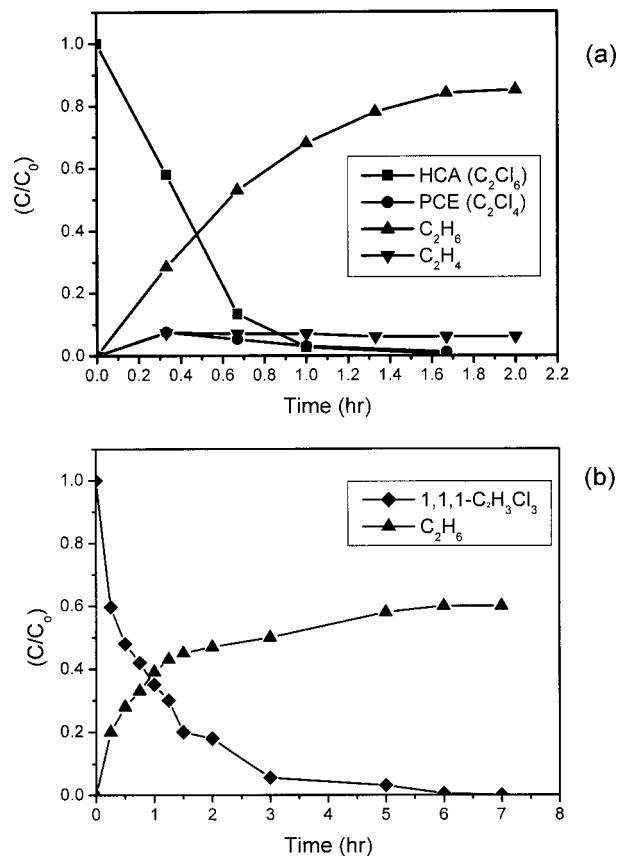


Fig. 1. Reactions of nanoscale Pd/Fe bimetallic particles (5 g/L) with: (a) 30 mg/L of hexachloroethane, and (b) 30 mg/L of 1,1,1-trichloroethane

Table 2. Summary of Bond Strength and One-Electron Reduction Potential for Chlorinated Ethanes and Surface-Area-Normalized Rate Constants

Chlorinated ethanes	Bond strength (kcal/mole)	One-electron reduction potential (V)	k_{SA} (L/h/m ²)
C ₂ Cl ₆	68.83	0.152	2.0 × 10 ⁻²
C ₂ HCl ₅	68.95	0.139	2.6 × 10 ⁻²
1,1,1,2-C ₂ H ₂ Cl ₄	70.19	0.077	2.1 × 10 ⁻²
1,1,2,2-C ₂ H ₂ Cl ₄	74.65	-0.175	8.8 × 10 ⁻³
1,1,1-C ₂ H ₃ Cl ₃	73.6	-0.031	5.4 × 10 ⁻³

tration of metal (g/L). In this study, a_s and ρ were 33.5 (m²/g) and 5(g/L), respectively. The values of k_{SA} (Table 2) were determined by applying Eqs. (3) and (4).

In this study, one-electron reduction potentials and bond strengths were used as the descriptors of correlation analysis. Data for the surface-area-normalized rate constants (k_{SA}), one-electron reduction potential (Arnold et al. 1999), and bond strength (Liu et al. 2000) for chlorinated ethanes are listed in Table 2. The correlation results of log-surface-area-normalized rate constant ($\ln [1/k_{SA}]$) versus one-electron reduction potentials and bond strength are illustrated in Fig. 2. The one-electron reduction potential was moderately ($r^2=0.598$) correlated with reaction rates, whereas a highly correlated relationship ($r^2=0.809$) between bond strength and reaction rate was obtained.

Correlation analysis as shown in Fig. 2 suggests that the rate of hydrodechlorination varies inversely with the bond strength. The C–Cl bond strength in 1,1,1-TCA is 73.6 kcal/mole which is

significantly higher than that of HCA at 68.8 kcal/mole. Hence the rate of 1,1,1-TCA transformation was slower than that of HCA. Similar trends can also be observed with other chlorinated ethanes.

Results obtained in this work are consistent with the study by Arnold et al. (1999) in which a moderate correlation exists between reaction rate and one-electron reduction potential for six chlorinated ethanes in reactions with zinc. For electrolytic dechlorination, the correlation between rate constants and bond strength was also excellent for chlorinated ethanes ($r^2 > 0.90$) (Liu et al. 2000).

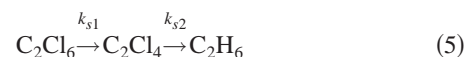
Although one-electron reduction potential and bond strength are often highly correlated to each other because both entail the cleavage of the carbon–halogen bond ($RX + e^- \rightarrow R \cdot + X^-$) (Scherer et al. 1998; Liu et al. 2000; Totten and Roberts 2001), Sometimes divergent results as shown in Fig. 2 are also possible. In general, there is a large uncertainty associated with the calculated values of one-electron reduction potential. Bond strength on the other hand, tends to be more accurate and has been suggested as a better descriptor for the correlation analysis (Totten and Roberts 2001).

Sequential Dechlorination

Many studies suggest that the reduction of chlorinated aliphatics especially biologically mediated reactions occur via a series of stepwise reactions, i.e., the dechlorination is accomplished by removing one chlorine at a time, from HCA to PCA, TeCA, TCA, DCA, then to chloroethene, finally to ethane. We have independently obtained rate constants for all the chlorinated ethanes so it may be possible to corroborate the conventional sequential hydrogenolysis pathway. However, invoking the stepwise reduction of HCA to ethane failed to explain our experimental results. Calculations based on independently obtained rate constants with the sequential dechlorination pathway would lead to a significant accumulation of DCA and a very low yield of ethane. Actual results shown in Fig. 1(a) show a high yield of ethane and no accumulation of DCA. Because of the low reactivity of DCA, direct hydrogenolysis of DCA to chloroethane was limited. It is therefore necessary to consider other route(s) for the formation of ethane.

β -Elimination

Transformation of highly chlorinated ethanes (chlorinated ethanes with an α, β pair of chlorine atoms) by zero-valent metals has been suggested to proceed via reductive β elimination (Arnold et al. 1999). The corresponding products from reductive β elimination of higher chlorinated ethanes were found in this study. For example, the appearances of PCE, TCE, and 1,1-DCE with yields between 7.5 and 15% were found in the transformation of HCA, PCA, and 1,1,1,2-TeCA. Based on the observed products and intermediates, one might consider reaction pathways for HCA transformation to ethane as follows:



where k_{s1} and k_{s2} =rate constants. Eq. (5) can be modeled using a set of ordinary differential equations

$$\frac{d[C_2Cl_6]}{dt} = -k_{s1}[C_2Cl_6] \quad (6)$$

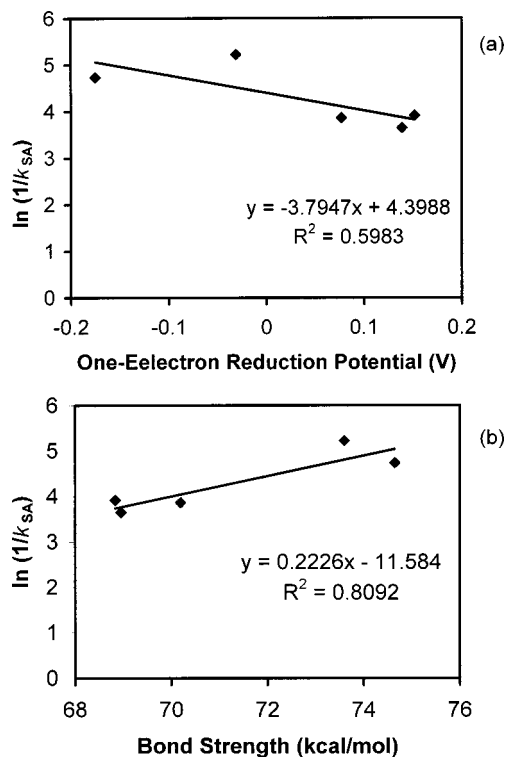


Fig. 2. Correlations of log-surface-area-normalized rate constants ($\ln [1/k_{SA}]$) with: (a) one-electron reduction potential and (b) bond strength for chlorinated ethanes

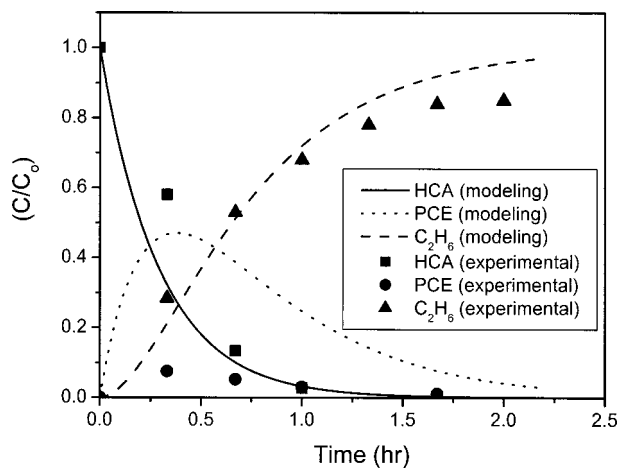


Fig. 3. Model simulation [Eq. (5)] and experimental results for hexachloroethane degradation

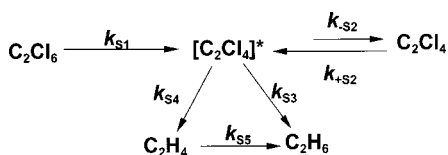
$$\frac{d[\text{C}_2\text{Cl}_4]}{dt} = +k_{S1}[\text{C}_2\text{Cl}_6] - k_{S2}[\text{C}_2\text{Cl}_4] \quad (7)$$

$$\frac{d[\text{C}_2\text{H}_6]}{dt} = +k_{S2}[\text{C}_2\text{Cl}_4] \quad (8)$$

The above differential equations were solved by using a *MAPLE V* software package. The rate constants of k_{S1} and k_{S2} can be determined independently from the reactions of HCA and PCE, respectively. k_{S1} was measured to be 3.43 h^{-1} (Table 1), while k_{S2} was 2.1 h^{-1} under identical conditions from our previous work (Lien and Zhang 2001). Simulation results and experimental data are presented in Fig. 3. It is apparent from the simulation that a substantial amount of PCE (47% at maximum) should have been detected if the reaction pathways shown in Eq. (5) governs. The actual yield of PCE was less than 10% throughout the experiment. We are fairly confident that the conflicting results between kinetic simulations and experiments cannot be attributed to analytic errors because the analytical method (GC-ECD) is very sensitive for PCE with a detection limit approaching $1 \mu\text{g/L}$. Consequently, it may imply that the elimination pathway as shown in Eq. (5) is probably not the major route of HCA dechlorination.

Surface Complex Model

We therefore propose a new reaction pathway as illustrated in Scheme 1 for the transformation of HCA. Our proposition builds on our experimental results as well as published observations from many other studies. The key element for our proposal is a surface transitional species. As stated above, reactions of chlorinated solvents with zero-valent metals are surface mediated (Weber 1996; Arnold and Roberts 2000). Surface-bound interme-



Scheme 1. Reaction pathways incorporating transition state in transformation of hexachloroethane

diates such as di- σ -bonded PCE resulting from reductive β elimination of PCE have been proposed (Arnold and Roberts 2000). The existence of a transition state during the transformation of chlorinated ethanes is supported by our correlation analysis. Taken together, the evidence, although indirect, suggests that the significance of surface intermediates to chlorinated ethane transformation needs to be explored.

The crucial step in the proposed reaction pathway is the formation of a transition state species $[\text{C}_2\text{Cl}_4]^*$, which could be the corresponding β -elimination product (di- σ -bonded PCE) during the reaction. Reduction of HCA to PCE was observed in this study. As noted earlier, PCE readily degraded to ethane in the presence of nanoscale Pd/Fe bimetallic particles (Lien and Zhang 2001). Therefore, if $[\text{C}_2\text{Cl}_4]^*$ exists during the HCA transformation, reactions between PCE and $[\text{C}_2\text{Cl}_4]^*$ should be reversible. In Scheme 1, two separate pathways are also considered for the formation of ethane: direct generation from the transition state, and also hydrogenation of ethylene.

The equations used to model the reactions illustrated in Scheme 1 are listed as follows:

$$\frac{d[\text{C}_2\text{Cl}_6]}{dt} = -k_{S1}[\text{C}_2\text{Cl}_6] \quad (9)$$

$$\frac{d[\text{C}_2\text{Cl}_4]}{dt} = -k_{+S2}[\text{C}_2\text{Cl}_4] + k_{-S2}[\text{C}_2\text{Cl}_4]^* \quad (10)$$

$$\begin{aligned} \frac{d[\text{C}_2\text{Cl}_4]^*}{dt} = & +k_{S1}[\text{C}_2\text{Cl}_6] + k_{+S2}[\text{C}_2\text{Cl}_4] - k_{-S2}[\text{C}_2\text{Cl}_4]^* \\ & - k_{S3}[\text{C}_2\text{Cl}_4]^* - k_{S4}[\text{C}_2\text{Cl}_4]^* \end{aligned} \quad (11)$$

$$\frac{d[\text{C}_2\text{H}_4]}{dt} = +k_{S4}[\text{C}_2\text{Cl}_4]^* - k_{S5}[\text{C}_2\text{H}_4] \quad (12)$$

$$\frac{d[\text{C}_2\text{H}_6]}{dt} = +k_{S3}[\text{C}_2\text{Cl}_4]^* + k_{S5}[\text{C}_2\text{H}_4] \quad (13)$$

The rate constants that can be measured directly were k_{S1} and k_{S2} as described above. The value of k_{S2} is the sum of k_{+S2} and k_{-S2} representing the forward and reverse reaction rate constants, respectively, in the transformation of PCE. The values of k_{+S2} , k_{-S2} , and other rate constants (i.e., k_{S3} , k_{S4} , and k_{S5}) were determined by simultaneously solving Eqs. (10)–(13) while fitting the model to experimental data. The best-fit results are shown in Fig. 4 and the best-fit values of k_{+S2} , k_{-S2} , k_{S3} , k_{S4} , and k_{S5} are provided in Table 3.

The validity of this proposed model was further evaluated by applying the rate constants to fit the experimental data of PCE transformation determined independently in our previous study (Lien and Zhang 2001). In the transformation of PCE, a small amount of ethylene ($<1\%$) was detected. Tetrachloroethylene was converted mostly to ethane (80%). Results for the simulation of ethane formation from the PCE degradation along with the experimental data are shown in Fig. 5. In this simulation, the rate constants that were applied included k_{+S2} , k_{-S2} , k_{S3} , k_{S4} , and k_{S5} . Although the rate of ethane formation is underestimated slightly by the model simulation, the rate constants determined from the HCA transformation fairly accurately explain the formation of ethane determined from the independent study of PCE transformation.

As shown in Fig. 4, the model calculations essentially captured all the major features of the experimental data of HCA dechlori-

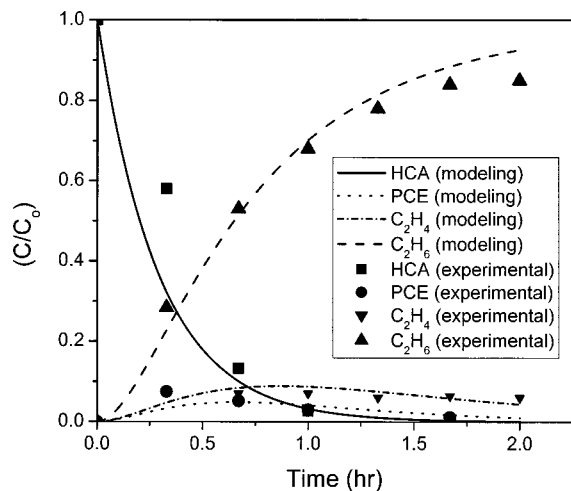


Fig. 4. Model simulation (based on Scheme 1) and experimental results for hexachloroethane degradation

nation after incorporating the transition state species and strengthens the hypothesis of a surface intermediate. Ethane production from direct transformation has the rate of 1 order of magnitude higher than that of ethylene hydrogenation. This suggests that the major route for ethane formation is likely to be the direct transformation of the surface intermediate (without the involvement of PCE) while the hydrogenation of ethylene to ethane is probably a minor reaction. In summary, the HCA transformation could consist of three independent reactions, HCA to ethane ($k_{s1}, k_{s3}, k_{s4}, k_{s5}$), HCA to PCE (k_{s1}, k_{s2}), and PCE to ethane ($k_{s2}, k_{s3}, k_{s4}, k_{s5}$).

The surface transition state can also explain other observations as well. Because of the lack of an α, β pair of chlorine atoms, 1,1,1-TCA does not undergo the β elimination. Studies have shown that transformation of 1,1,1-TCA with zero-valent zinc proceeds via concurrent α elimination and hydrogenolysis (Arnold et al. 1999). In this work, however, hydrogenolysis of 1,1,1-TCA to 1,1-DCA could account for less than 1% of the 1,1,1-TCA degradation as no α -elimination product (i.e., 1,1-DCE) was observed. Moreover, sequential hydrogenolysis of 1,1,1-TCA to ethane is ruled out because the near-zero reactivity of 1,1-DCA essentially inhibits the stepwise reaction. Considering the effect of surface intermediates, it seems reasonable that a surface transition state or intermediate may also play a role in reactions of 1,1,1-TCA.

Table 3. Experimental and Fitted Reaction Rate Constants for Pathways shown in Scheme 1

Symbol	Rate constants (h^{-1})	Portion of pathway	Method
k_{s1}	3.4	$C_2Cl_6 \rightarrow [C_2Cl_4]^*$	Experimental
k_{s2}	2.1	$C_2Cl_4 \leftrightarrow [C_2Cl_4]^*$	Experimental
k_{s2}	2.6	$[C_2Cl_4]^* \rightarrow C_2Cl_4$	Fitted
k_{s2}	0.5	$C_2Cl_4 \rightarrow [C_2Cl_4]^*$	Fitted
k_{s3}	2.5	$[C_2Cl_4]^* \rightarrow C_2H_6$	Fitted
k_{s4}	0.2	$[C_2Cl_4]^* \rightarrow C_2H_4$	Fitted
k_{s5}	2.0	$C_2H_4 \rightarrow C_2H_6$	Experimental

Note: $k_{s2} = k_{s2} + k_{s2}$.

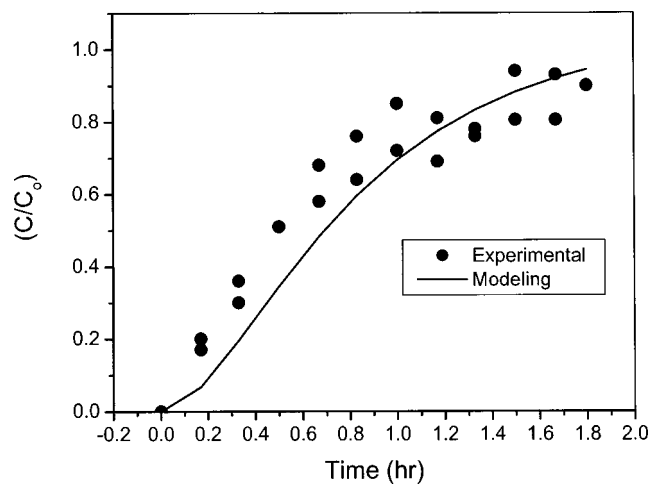
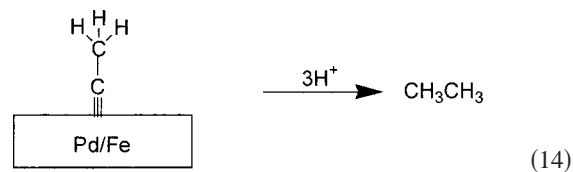


Fig. 5. Comparison of model simulation and experimental observations of ethane formation from tetrachloroethylene degradation; model parameters were obtained from hexachloroethane experiment

The formation of surface intermediates on metal surfaces has been observed in the reactions of many chlorinated organic compounds and hydrocarbons with metals in the gas phase. Hydrocarbon moieties such as alkyl, carbene, and carbyne have been found using various surface-sensitive techniques (Baltruschat et al. 1993; Bent 1996). In aqueous solution, the formation of hydrocarbon moieties has also been reported. For example, carbene, and carbyne species was observed in the transformation of chlorinated methanes (Zaera 1995). In the case of trichloroethanes, formation of surface ethylidyne (CCH_3) has been reported on transition metal surfaces in both gas and aqueous phase reactions (Müller et al. 1997; Hsiao et al. 1998). The surface ethylidyne has been identified in the transformation of 1,1,1-TCA to ethane by a palladium electrode in aqueous solution (Hsiao et al. 1998). In this study, the transformation of 1,1,1-TCA resulting in substantial production of ethane could be explained by the formation of ethylidyne as a surface intermediate. Through ethylidyne, ethane could be readily formed during the 1,1,1-TCA transformation without involving the sequential reactions that would result in the formation of lesser chlorinated ethanes as shown in the following equation:



No suitable analytic method is currently available to obtain direct evidence of the proposed surface-bound reaction intermediate. Nonetheless the final product distribution and kinetic calculations support the hypothesis that a surface-mediated dechlorination leads to the formation of a transition species at the surface. Reaction mechanisms such as elimination and hydrogenolysis can account for less than 20% of the final products from HCA dechlorination. Using the proposed model, hydrodechlorination of chlorinated ethanes with a high yield of ethane and low yields of lesser chlorinated intermediates, can be fully explained by the surface intermediate.

Acknowledgments

This work is supported partially by U.S. Environmental Protection Agency (USEPA) Grant No. 829625 and by a CAREER award to W.Z. from U.S. National Science Foundation (NSF) Grant No. 9983855.

References

- Arnold, W. A., Ball, W. P., and Roberts, A. L. (1999). "Polychlorinated ethane reaction with zero-valent zinc: Pathways and rate control." *J. Contam. Hydrol.*, 40, 183–200.
- Arnold, W. A., and Roberts, A. L. (1998). "Pathways of chlorinated ethylene and chlorinated acetylene reaction with Zn(0)." *Environ. Sci. Technol.*, 32, 3017–3025.
- Arnold, W. A., and Roberts, A. L. (2000). "Pathways and kinetics of chlorinated ethylene and chlorinated acetylene reaction with Fe(0) particles." *Environ. Sci. Technol.*, 34, 1794–1805.
- Baltruschat, H., Beltowska-Brzezinska, M., and Dülberg, A. (1993). "Reactions of halogenated hydrocarbons at platinum group metals. Part I: A DEMS study of the adsorption of CH_3CCl_3 ." *Electrochim. Acta*, 38, 281–284.
- Bent, B. E. (1996). "Mimicking aspects of heterogeneous catalysis: Generating, isolating, and reacting proposed surface intermediates on single crystals in vacuum." *Chem. Rev. (Washington, D.C.)*, 96, 1361–1390.
- Burrow, P. D., Aflatooni, K., and Gallup, G. A. (2000). "Dechlorination rate constants on iron and the correlation with electron attachment energies." *Environ. Sci. Technol.*, 34, 3368–3371.
- Campbell, T. J., Burris, D. R., Roberts, A. L., and Wells, J. R. (1997). "Trichloroethylene and tetrachloroethylene reduction in a metallic iron-water-vapor batch system." *Environ. Sci. Technol.*, 16, 625–630.
- Elliott, D. W., and Zhang, W. X. (2001). "Field assessment of nanoscale bimetallic particles for groundwater treatment." *Environ. Sci. Technol.*, 35, 4922–4926.
- Fennelly, J. P., and Roberts, A. L. (1997). "Reaction of 1,1,1-trichloroethane with zero-valent metals and bimetallic reductants." *Environ. Sci. Technol.*, 32, 1980–1988.
- Glavee, G. N., Klabunde, K. J., Sorensen, C. M., and Hadjipanayis, G. C. (1995). "Chemistry of borohydride reduction of iron(II) and iron(III) ions in aqueous and nonaqueous media. formation of nanoscale Fe, FeB, and Fe_2B powders." *Inorg. Chem.*, 34, 28–35.
- Grittini, C., Malcomson, M., Fernando, Q., and Korte, N. (1995). "Rapid dechlorination of polychlorinated biphenyls on the surface of a Pd/Fe bimetallic system." *Environ. Sci. Technol.*, 29, 2898–2900.
- Hsiao, G. S., Erley, W., and Ibach, H. (1998). "Photodecomposition of 1,1,2-trichloroethane: Spectroscopic evidence for vinyl formation on Pt(111)." *Surf. Sci.*, 396, 422–430.
- Johnson, T. L., Scherer, M. M., and Tratnyek, P. G. (1996). "Kinetics of halogenated organic compound degradation by iron metal." *Environ. Sci. Technol.*, 30, 2634–2640.
- Lien, H.-L., and Zhang, W. X. (1999). "Transformation of chlorinated methanes by nanoscale iron particles." *J. Environ. Eng.*, 125(11), 1042–1047.
- Lien, H.-L., and Zhang, W. X. (2001). "Nanoscale iron particles for complete reduction of chlorinated ethenes." *Colloids Surf., A*, 191, 97–106.
- Liu, Z., Betterton, E. A., and Arnold, R. G. (2000). "Electrolytic reduction of low molecular weight chlorinated aliphatic compounds: structural and thermodynamic effects on process kinetics." *Environ. Sci. Technol.*, 34, 804–811.
- Matheson, L. J., and Tratnyek, P. G. (1994). "Reductive dehalogenation of chlorinated methanes by iron metal." *Environ. Sci. Technol.*, 28, 2045–2053.
- Müller, U., Dülberg, A., Stoyanova, A., and Baltruschat, H. (1997). "Reactions of halogenated hydrocarbons at Pt-group metals—II. On the adsorption rate at Pt and Pd electrodes." *Electrochim. Acta*, 42, 2499–2509.
- Orth, S. W., and Gillham, R. W. (1996). "Dechlorination of trichloroethene in aqueous solution using Fe(0)." *Environ. Sci. Technol.*, 30, 66–71.
- Roberts, A. L., Totten, L. A., Arnold, W. A., Burris, D. R., and Campbell, T. J. (1996). "Reductive elimination of chlorinated ethylenes by zero-valent metals." *Environ. Sci. Technol.*, 30, 2654–2659.
- Scherer, M. M., Balko, B. A., Gallagher, D. A., and Tratnyek, P. G. (1998). "Correlation analysis of rate constants for dechlorination by zero-valent iron." *Environ. Sci. Technol.*, 32, 3026–3033.
- Squillace, P. J., Moran, M. J., Lapham, W. W., Price, C. V., Clawges, R. M., and Zogorski, J. S. (1999). "Volatile organic compounds in untreated ambient groundwater of the United States, 1985–1995." *Environ. Sci. Technol.*, 33, 4176–4187.
- Totten, L. A., and Roberts, A. L. (2001). "Calculated one- and two-electron reduction potentials and related molecular descriptors for reduction of alkyl and vinyl halides in water." *Crit. Rev. Environ. Sci. Technol.*, 31, 175–221.
- United States Environmental Protection Agency (USEPA). (1979). "Water-related environmental fate of 129 priority pollutants. Volume II: Halogenated aliphatic hydrocarbons, halogenated ethers, monocyclic aromatics, phthalate esters, polycyclic aromatic hydrocarbons, nitrosamines, and miscellaneous compounds." *EPA-440/4-79-029B*, Office of Water Planning and Standards, Washington, D.C.
- Wang, C. B., and Zhang, W. X. (1997). "Nanoscale metal particles for dechlorination of TCE and PCBs." *Environ. Sci. Technol.*, 31, 2154–2156.
- Weber, E. J. (1996). "Iron-mediated reductive transformations: Investigation of reaction mechanism." *Environ. Sci. Technol.*, 30, 716–719.
- Zaera, F. (1995). "An organometallic guide to the chemistry of hydrocarbon moieties on transition metal surfaces." *Chem. Rev. (Washington, D.C.)*, 95, 2651–2693.
- Zhang, W. (2003). "Nanoscale iron particles for environmental remediation: An overview." *J. Nanopart. Res.*, 5, 323–332.
- Zhang, W. X., Wang, C. B., and Lien, H.-L. (1998). "Treatment of chlorinated organic contaminants with nanoscale bimetallic particles." *Catal. Today*, 40, 387–395.